Tellus (1998), 50B, 543–554
Printed in UK – all rights reserved

TELLUS
ISSN 0280–6509

The direct radiative effect of smoke aerosols on atmospheric absorption of visible sunlight

By ZHANQING LI[1]*, and LINHONG KOU[2], [1]*Canada Centre for Remote Sensing, Ottawa, Ontario, Canada;* [2]*Intermap Technologies, Ottawa, Ontario, Canada*

(Manuscript received 10 March 1998; in final form 22 July 1998)

ABSTRACT

Smoke aerosol has a significant effect on the atmospheric radiation budget due to its strong absorbing properties. Observational studies of the smoke radiative effect (SRE) usually suffer from a shortage of in-situ measurements of aerosol optical properties. This study introduces a new approach to determine SRE, i.e. the amount of solar energy absorbed in the atmosphere, under any sky conditions, using satellite and surface measurements. The method requires no observation of aerosol optical properties. It is based on a satellite inversion algorithm that retrieves surface net solar radiation in the visible spectrum (400–700 nm). The algorithm was first validated under a variety of sky conditions ranging from clear, to smoky, and to cloudy skies. It is found that the accuracy of retrieval is affected only by absorbing aerosols such as smoke. Without correction for this effect, the difference between observed and estimated fluxes is a good estimate of SRE. Following this approach, instantaneous, daily and monthly mean SRE were computed, over a study site in the remote boreal forest region of western Canada, where fire activities dominate the variation of aerosol loading during the summer season. The monthly and daytime mean SRE reaches a maximum value of 26.0 W m^{-2} during a period of active burning in July 1994, in comparison to a total deduction of solar radiation budget by both clouds and smoke of 76.7 W m^{-2} at the surface within the specified visible solar spectral spectrum.

1. Introduction

As a potential offsetting agent to the greenhouse effect, aerosols are receiving increasing attention in the atmospheric science community. Nevertheless, our knowledge of the impact of aerosols on radiation and climate is still rather poor and falls well behind our knowledge of the greenhouse effect. For example, the majority of estimates of direct radiative forcing (DRF) due to greenhouse gases are within 15%, whereas those for aerosols differ by at least a factor of two (IPCC, 1995). Due to the complex interactions between aerosols and the physical and chemical components of the Earth's climate system, our understanding of their role in climate change is beset with uncertainties (Schwartz and Andreae, 1996; Hansen et al., 1997). Since aerosols are situated in the lower boundary layer, aerosol shortwave (SW) DRF is usually much larger than its long wave (LW) counterpart. This study is thus confined to SW only.

To date, much work on the aerosol radiative effect has concentrated on sulfate aerosols (Charlson and Heintzenberg, 1995). More attention needs to be paid to other types of aerosols such as carbonaceous aerosols (Haywood and Shine, 1995). Sulfate aerosols attenuate solar radiation primarily by scattering, while carbonaceous aerosols absorb, as well as scatter solar radiation.

* Corresponding author.
Address: CCRS, 588 Booth Street, Ottawa, Canada, K1A 0Y7, email: zhanqing.li@ccrs.nrcan.gc.ca.

As a result, sulfate aerosols usually have a cooling effect at both the top of the atmosphere (TOA) and at the surface, but have little or no effect on the heating rate of the atmosphere. The influence of carbonaceous aerosols is more complex, cooling at the surface, warming in the atmosphere and uncertain at the TOA. The sign of the DRF at the TOA is dictated by the magnitude of the warming effect in the atmosphere. Therefore, when studying carbonaceous aerosols, the radiative effect in the atmosphere is of critical value. So far, few studies have addressed this effect.

Smoke aerosol from biomass burning is a major component of carbonaceous aerosols. The large variability and lack of in-situ measurements in the loading and optical properties of smoke aerosols pose considerable difficulties in studying their radiative effects. Consequently, the current estimates of global mean DRF due to smoke aerosols differ by a factor of about three (Penner et al., 1992; Chylek and Wong, 1995; Hobbs et al., 1997), which is considered as the range of uncertainty in our current understanding (IPCC, 1995).

There are many studies concerning the radiative effect of smoke in the tropics (Christopher et al., 1996; Kaufman and Fraser, 1997; Li, 1998), but few studies have been reported in other regions. For example, boreal forest fires occur so often and extensively that they warrant more attention (Stocks, 1996; Li et al., 1997a). Another limitation in the studies of SRE is that they were confined to cloudless days. This is because measurements of smoke properties are usually only available for clear skies.

This study introduces a novel approach to determining the amount of solar energy absorbed in the atmosphere in the visible wavelengths (400 to 700 nm), which is simply referred to as the smoke radiative effect (SRE) in order to differentiate it from the conventional definition of DRF. Note that DRF usually denotes the net change in the radiation budget at the TOA due to both the scattering and absorbing of aerosols. The method proposed here is valid under both clear and cloudy conditions. The approach requires no cloud/smoke discrimination, nor does it require observations of smoke properties. The study is concerned with fires that occurred in a boreal forest region in western Canada.

The methodology and data sets employed are discussed in Section 2 and 3 respectively. Section 4 validates a satellite-based retrieval algorithm that is essential to the methodology. Section 5 computes SRE and compares it with the total radiative effect of clouds and smoke at the surface. Conclusions are given in Section 6.

2. Methodology

The methodology involves a satellite algorithm that retrieves solar radiation in the visible region from 400 nm to 700 nm (Li and Moreau, 1996). This radiation is often referred to as photosynthetically active radiation (PAR), as it is the radiation in this spectral region that governs the photosynthesis of vegetation growth. The unique advantage of using this algorithm is that retrieval is affected by very few atmospheric parameters, most notably the absorbing aerosols. Without the presence of absorbing aerosols, clouds have negligible absorption in the PAR wavelengths and so do conservative aerosols, water vapour and other atmospheric constituents. Weak absorption due to ozone and oxygen is taken into account by the algorithm. Consequentely, the difference between observed and estimated surface PAR radiation is affected mainly by the atmospheric absorption of absorbing aerosols. In remote areas of the boreal forests in northern Canada, the loading of background aerosols is so low that its fluctuation in the summer season is caused primarily by forest fires (Markham et al., 1997). Therefore, we can further attribute the difference to the smoke radiative effect in the atmosphere.

The algorithm developed by Li and Moreau (1996) is basically a coupling of the relationship between TOA-reflected and surface-absorbed visible radiation for a fixed solar zenith angle (SZA). The coupling exists because an increase in the amount of cloud and aerosol leads to an increase in the flux reflected back to space and accordingly, diminishes the flux absorbed at the surface. The difference between changes in TOA and surface radiative fluxes depends on atmospheric absorption. For conservative scattering media such as clouds and sulfate aerosols, changes at the TOA and at the surface should be identical in magnitude but of the opposite sign. For absorbing media such as smoke, the relationship is dependent on the optical properties of the medium (e.g., single scattering albedo and optical depth). On the basis

of radiative transfer calculations, Li and Moreau (1996) developed the following parameterizations to determine the net PAR absorbed at the surface (APAR) from satellite observed visible albedo (ρ_{TOA}).

$$\mathrm{APAR} = [\alpha(\mu, O_3, \tau_e) - \beta(\mu, O_3, \tau_e)] \times \rho_{TOA}\mu d^{-2}\,\mathrm{PAR}_{TOA}, \quad (1)$$

$$\alpha(\mu, O_3, \tau_e) = -0.015 + \exp(-0.05O_3\mu^{-1}) - 0.168\tau_e \times [\exp(-3\mu^2) + 1], \quad (2)$$

$$\beta(\mu, O_3, \tau_e) = \exp(0.083O_3) - 0.168\tau_e (1.21 - 0.348\mu) \times [\exp(-3\mu^2) + 1], \quad (3)$$

$$\tau_e = \tau_a((1 - \omega_a)/0.109)^{0.845}, \quad (4)$$

where μ is the cosine of the SZA. O_3 is the amount of ozone in centimeter-atm. τ_a and ω_a are aerosol optical thickness and single scattering albedo respectively. τ_e denotes effective aerosol optical thickness. It follows from (4) that τ_e is equal to zero for conservative aerosols ($\omega_a = 1$), regardless of its optical thickness. d is the sun-earth distance in astronomical units. PAR_{TOA} is the incident radiation between 400–700 nm at the TOA for a mean sun-earth distance ($d = 1$), which is set to be 544 W m^{-2} according to the extraterrestrial solar irradiance data of Iqbal (1983).

Until now, the algorithm has been tested with a limited amount of AVHRR measurements (Li et al., 1997b). A more comprehensive validation is conducted here with a large volume of GOES (Geostationary Operational Environmental Satellite) data under a variety of conditions: clear, smoky and cloudy skies. For testing the algorithm, aerosol measurements are required, but for determining SRE they are not. Issues related to the uncertainties and corrections of surface and satellite measurements, and their match in time and space have been addressed in Li et al. (1997b). They are thus omitted here, except for new problems arising from the use of different data sets.

3. Data

All data employed in this study were acquired during the Boreal Ecosystem–Atmosphere Study (BOREAS). BOREAS is an international field experiment aiming to improve understanding of the exchange of radiative energy, sensible heat, water, CO_2 and trace gases between the boreal forest and the atmosphere (Sellers et al., 1995). The experiment took place in the boreal forest regions of Saskatchewan and Manitoba, Canada between 1994 and 1996. Full-fledged intensive field campaigns were conducted in 1994 during which comprehensive meteorological, hydrological and ecological data were obtained by international science teams. Most of the variables were measured at observational towers located in the middle of uniform forest stands of various types. The measurements represent spatial averages over areas of several square kilometres. These ground-based observations were matched to satellite data. Measurements made at a young jack pine site (YJP) (55.903°N, 98.288°W) in the northern study area (NSA) were employed in this study. The most complete data sets required for this investigation were available at this site. Both downwelling and upwelling PAR fluxes and aerosol were observed.

TOA visible albedo was observed by the GOES satellite every half hour. This permitted an extensive validation of the algorithm, and calculation of daily and monthly mean SRE. The spatial resolution of the data is approximately 0.83×1.78 km^2 in the area of the BOREAS study region (Gu and Smith, 1997). The band width of the GOES visible channel is approximately 0.54–0.67 μm. Calibration of the GOES data was based on Minnis et al. (1995). It was validated against data from the Scanner for Radiation Budget (ScaRaB) (Trishchenko and Li, 1998):

$$R = 0.00424D^2 + 0.00059, \quad (5)$$

where R denotes radiance (Wm^{-2} sr^{-1}) and D is a 6-bit digital count. Note that the original GOES-7 data are 8-bit instead of 6-bit, which results in a loss of accuracy of about 0.012 in terms of albedo.

In order to collocate GOES pixels with the BOREAS towers, the satellite data need to be registered correctly. Provisional geo-referencing information associated with GOES imagery was found to be erroneous with respect to the Canadian federal topographical database. The accuracy of GOES geo-referencing deteriorates with increasing latitude. Near the northern edges of the GOES images, the pixel location was off by about 11 km. In the area of the NSA where the research was conducted, the error was about 8 km. Using some ground control points obtained from

high-resolution image chips, the GOES pixels were re-registered around the NSA by shifting 4 pixels southward and 3 pixels westward. The precision of re-registration is better than the size of a pixel.

In order to understand the effect of smoke and to test the algorithm, information on fire activities is essential. Both satellite and surface measurements convey such information. The hot spots due to forest fires have been successfully detected using AVHRR data over the Canadian boreal forests (Li et al., 1997a). The summer of 1994 was a very active fire season. The nearest fires were only a few kilometres north of the observation site. Depending on wind direction, fires can seriously affect PAR measurements. Major fire events commenced in June, peaked in July and continue until the late summer of 1994. Although GOES-7 was not equipped to determine fire spots because it lacks a mid-infrared channel, smoke is clearly visible on GOES images if there are no clouds. Moreover, the high-frequency (every 30 min) of GOES images allows the tracing of smoke more readily than from daily AVHRR images. All the daytime GOES images were inspected to determine sky conditions.

Fire smoke can be quantified by the measurements of aerosol optical thickness. Aerosol observations were made continuously with a photometer at the YJP site in the NSA by Markham et al. (1997). They noted that aerosol optical thickness was heavily influenced by forest fires in 1994. Typical values of aerosol optical thickness were less than 0.1 in the absence of fires, but increased up to 5.0 when fires occurred nearby. There were two major limitations in the aerosol data: the absence of single scattering albedo measurements and the restriction to clear skies. Measurements of aerosol properties for boreal fire made by Radke et al. (1988) suggest a magnitude of single scattering albedo of approximately 0.9 at 550 nm. This value is very close to the continental model aerosol defined in WCP-112 (1986). By necessity, the continental model aerosol was assumed in this investigation, although the optical properties of smoke may vary with burning conditions.

4. Comparison between observation and estimation

Estimation of APAR was done using eqs. (1)–(4) with satellite-observed TOA albedo as a driving input parameter. If aerosol measurements were available, two sets of APAR outputs were produced: one with, and one without aerosol correction, by using actual measurements of aerosol optical thickness and $\tau_e = 0$, respectively. To substantiate the argument that the difference between estimated and observed APAR without aerosol correction approximates SRE, a series of comparisons were made. Benchmark cases of clear, smoky and cloudy skies are shown first, followed by comparisons for all sky conditions.

Fig. 1 shows the comparison for two clear days, 8 June and 12 July, together with the diurnal variations of aerosol optical thickness. Note that during the two days, fires did not abate, but simply no smoke affected the observation site. In fact, two plumes are discernible on the 8 June image that were blowing eastward away from, rather than southward towards the observation site located near the southern bound of the image. Consequently, a small aerosol optical thickness ranging from 0.035 to 0.075 was measured, which more or less represents the background aerosol loading in this region and season without fire events. Due to the small amount of aerosol, the two sets of estimation are similar and very close to observational values. The estimates with aerosol correction are slightly better than those without the correction. The diurnal variations of observed APAR are well reproduced by the satellite estimation. The mean and standard deviation of the differences between observed and estimated APAR with aerosol correction are just -0.92 and $10.0\ \mathrm{W\ m^{-2}}$ for 8 June, and 7.0 and $12.5\ \mathrm{W\ m^{-2}}$ for 12 July, respectively.

Fig. 2 presents the results for two smoky days: 2 July and 30 July, 1994. 2 July shows a smaller but more variable aerosol loading due to changes in wind direction, whereas 30 July displays a more even coverage of heavy smoke. The estimates of APAR without aerosol correction are considerably larger than the observed values, but those with the correction fall in very good agreement with observations. For example, the comparison for 30 July with aerosol correction is as good as for 8 June in terms of both mean and standard differences.

When clouds were present, there were no reliable measurements of aerosol optical thickness. Yet, the effect of smoke is generally much reduced due to the shielding effect of clouds that are

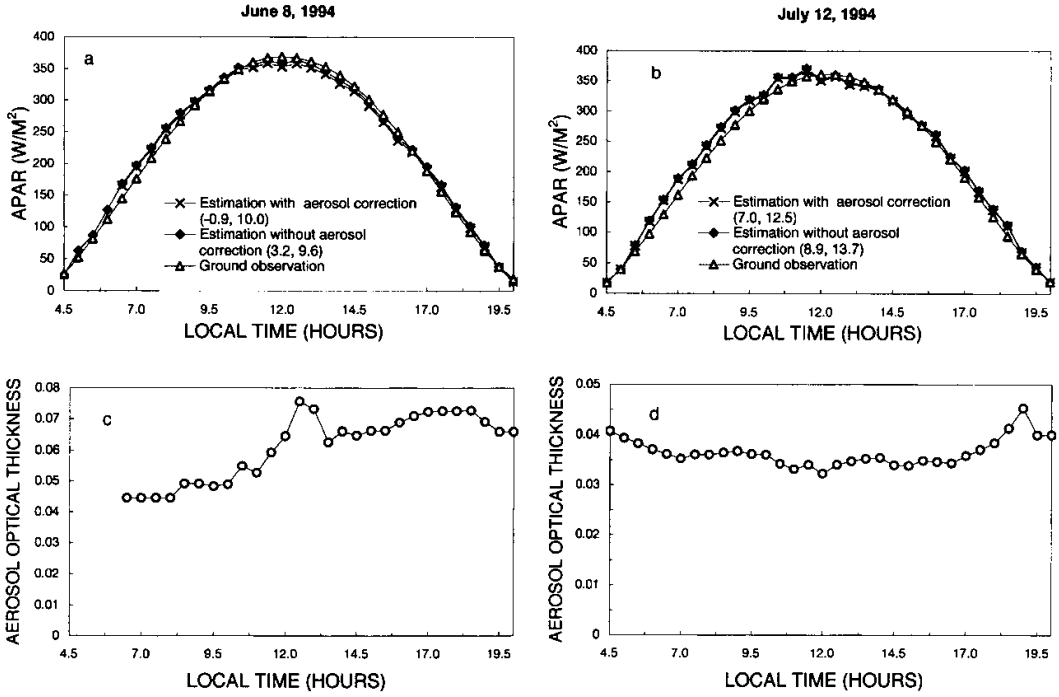

Fig. 1. Comparison between observed and estimated diurnal variation of APAR for two clear days, 8 June (**a**) and 12 July (**b**), 1994. The estimation was performed both with and without aerosol correction. Aerosol optical thickness for the two days is plotted in (**c**) and (**d**). Numbers in the parentheses of the panels (**a**) and (**b**) denote the mean (first number) and standard (second number) deviation of the differences between observed and estimated APAR.

situated usually above a smoke layer. Thus, no aerosol correction was applied in the estimation of APAR under cloudy conditions. Fig. 3 presents comparisons for four cloudy days, some having short periods of clear breaks. Relative to the clear sky comparisons shown above, the comparisons for cloudy sky exhibit more scattering, but the diurnal trends of observed APAR are again very well reproduced by satellite-based estimation. The relatively large deviation of estimated APAR from observations stems from greater uncertainty in matching between satellite and surface observations under cloudy conditions than under clear ones (Li et al., 1997b). Since clouds are usually non-uniform, ground-based PAR measurements may not represent aerial mean PAR as inferred from satellite measurements. Nevertheless, the comparisons are good in general, especially in terms of mean differences. It should be noted that there is a slight overestimation of the APAR values. This is most likely caused by the existence of a certain amount of aerosol inside the cloud layers.

Comparisons for all days are presented in Fig. 4. Fig. 4a is a comparison without aerosol correction for all the data that were matched. Fig. 4b is the same as Fig. 4a but for a subset of the data that have simultaneous measurements of aerosol optical thickness, but no aerosol correction was applied. Fig. 4c is the same as Fig. 4b but with aerosol correction. The comparison between Figs. 4a, b suggests that the systematic difference be caused primarily under clear-sky conditions. Such a difference is removed almost completely with aerosol correction, as is shown in Fig. 4c.

5. Determination of smoke direct radiative forcing

The above comparisons suggest that the satellite inversion algorithm of Li and Moreau (1996) be

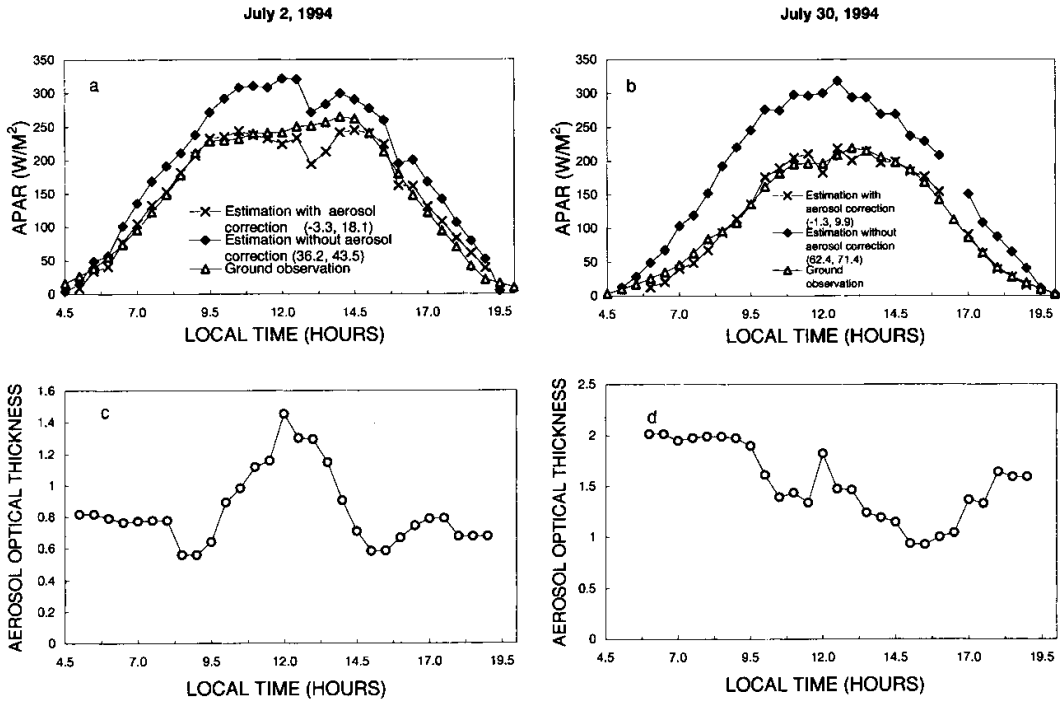

Fig. 2. Same as Fig. 1 except for 2 smoky days on 2 July (**a**) and 30 July (**b**), 1994.

able to retrieve surface APAR under any sky conditions, when aerosol measurements are available. Since the accuracy of retrieval is determined largely by the influence of absorbing aerosols, differences between estimated and observed APAR (the former minus the latter) *without* aerosol correction can be considered as an approximate estimate of the amount of solar energy absorbed by smoke, namely, the SRE. Given that the optical thickness of background aerosols is usually less than 0.1 in this region (Markham et al., 1997), a mean value of 0.05 is assumed to account for its influence on the estimation of APAR. Discrepancies between the resulting estimates of APAR and APAR observations are attributed, in principle, to SRE. In practice, however, the difference contains errors due to other factors such as the mismatch of satellite and surface measurements and uncertainties in the input data (Li et al., 1997b). Since these errors are of random nature, they can be eliminated or lessened by averaging. This method bypasses the difficulties in obtaining aerosol optical properties.

Instantaneous aerosol SRE was computed every half-hour from satellite and surface measurements. Daily and monthly mean SRE were then derived from instantaneous values. Fig. 5 plots the variations of mean SRE averaged over 24 h and over daytime only, in comparison with daytime mean aerosol optical thickness from 24 May to 9 September, 1994. Note that aerosol measurements were interrupted by the occurrence of clouds. Mean aerosol optical thickness was computed only for days having more than 10 measurements. A strong day-to-day variation in SRE is seen, ranging from near zero to larger than 60 W m^{-2} for daytime means and 40 W m^{-2} for daily means. The few negative values of SRE are a manifestation of the artifacts caused mainly by mismatching satellite and surface observations. Each peak value of aerosol optical thickness corresponds to a local maximum of SRE.

The monthly mean values of SRE are given in Fig. 6. In July, the daily mean was 17 W m^{-2} and daytime mean was 26 W m^{-2}. These values are halved for May and June. Given that the observed values of monthly daytime mean APAR for the months of May to September are equal to 152.9,

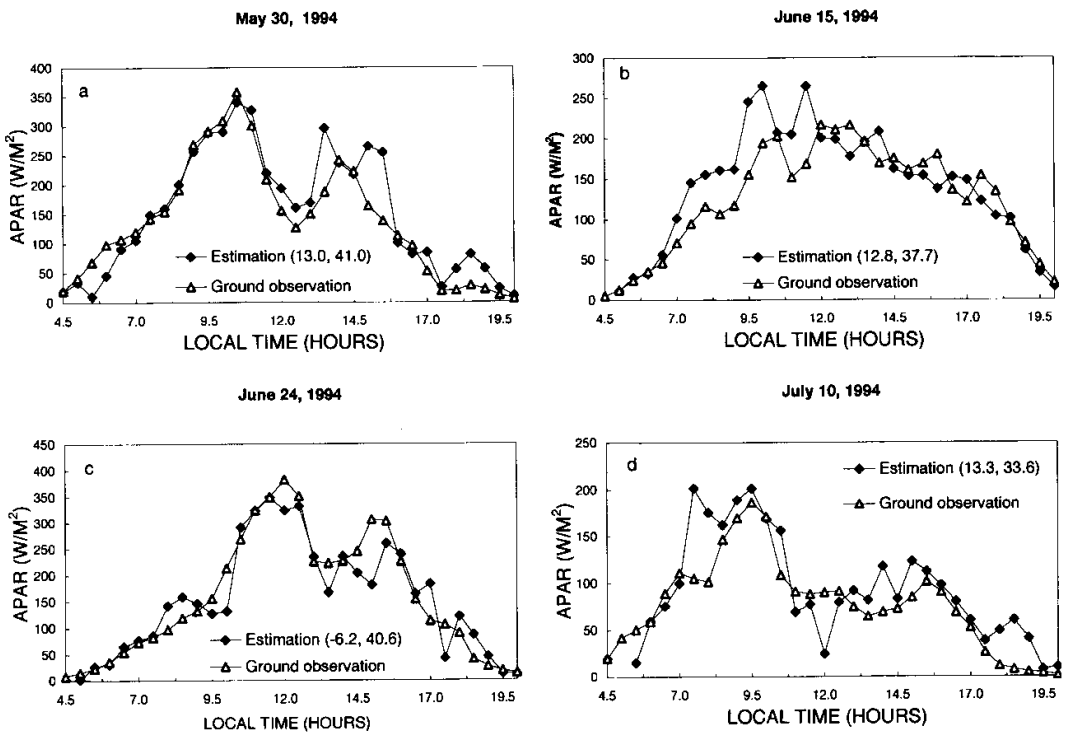

Fig. 3. Comparison between observed and estimated APAR for 4 cloudy days: 30 May (**a**),15 June (**b**), 24 June (**c**) and 10 July (**d**), 1994. No correction was made for aerosol effects.

168.1, 132.6, 110.7 and 96.4 W m^{-2}, the radiative effect of smoke aerosols is quite significant. Also included in the figure are the standard differences of these monthly mean values, as estimates of the uncertainties in monthly mean SRE. They were calculated by

$$\Delta\mathrm{SRE} = \frac{\delta\mathrm{SRE}}{\sqrt{N}}, \qquad (6)$$

where ΔSRE denotes the standard deviation of monthly mean SRE, and δSRE expresses the standard deviation of instantaneous SRE. N is the number of instantaneous estimates of SRE included in the calculation of monthly mean SRE.–68–ΔSRE ranges from 2.95 in May to 1.49 in July.

To put these estimates of SRE in the atmosphere in perspective, the total radiative effect (TRE) in the same spectral band (PAR) at the surface due to both clouds and aerosols including smoke was calculated. TRE is defined as the difference in the net radiative fluxes (down–up components) between all sky conditions and clear sky conditions. Note that TRE at the surface is altered not only by the absorbing effect of smoke in the atmosphere as denoted by SRE here, but also by the scattering effect of cloud and all aerosol particles. Daytime mean TRE can be determined as follows (c.f. Fig. 7). First, surface observed APAR is plotted against the cosine of the SZA. Second, clear sky measurements with low aerosol loading (<0.1) were identified according to surface and satellite observations. From these, a linear regression of APAR as a function of cos(SZA) is derived. It follows from Fig. 7 that the regression line is above most data points except for a few scattered ones. These values beyond the clear sky regression line were actually observed with a few scattered clouds. These clouds did not obscure the direct sunlight, but rather produced extra diffuse photons from their edges, leading to higher than clear sky values. Instantaneous TRE was determined as the difference between observed APAR given by the data points and the estimates of clear sky values

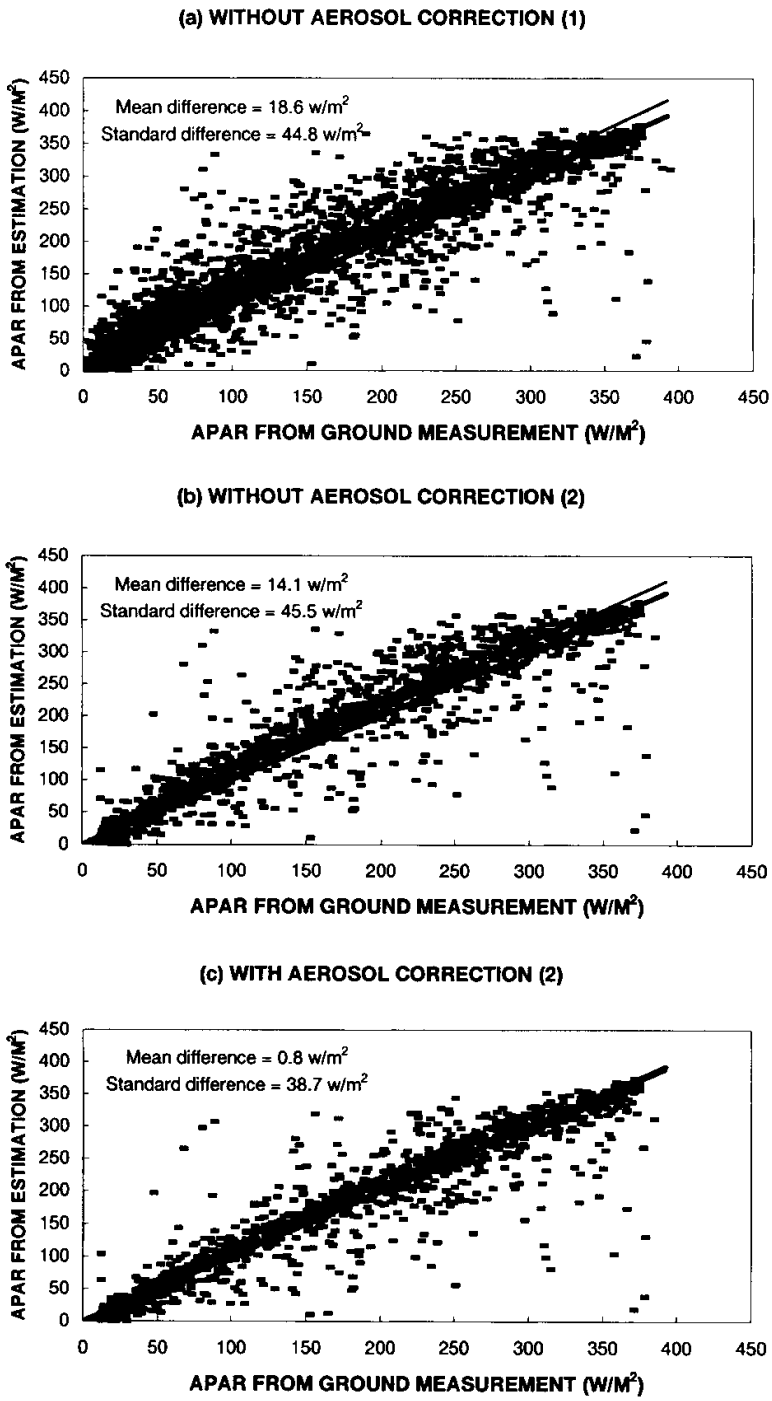

Fig. 4. Comparison between observed and estimated APAR. Plot (**a**) shows all matched data from 24 May to 9 September 1994, without aerosol correction. Plot (**b**) is the same as plot (**a**) but contains only the data having measurements of aerosol optical thickness. Plot (**c**) is the same as plot (**b**) but with aerosol correction. The thick and thin lines are 1:1 and regression lines, respectively.

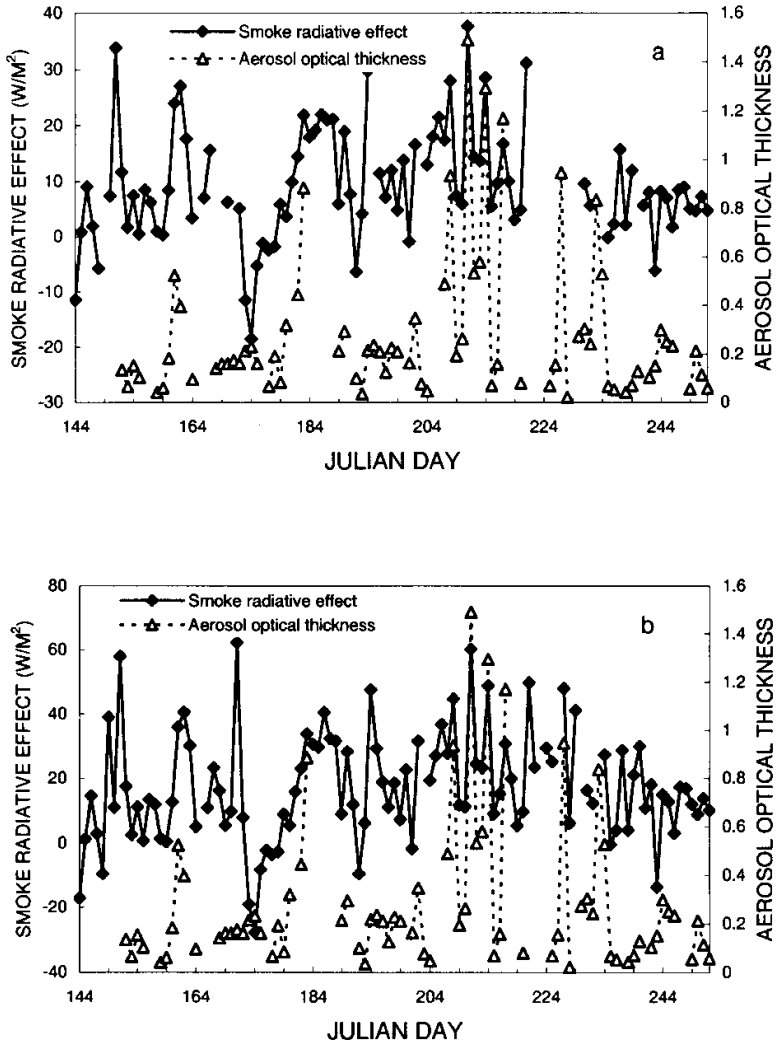

Fig. 5. Day-to-day variation of the daily mean value of SRE (**a**) and daytime mean value of SRE (**b**) with reference to daily mean value of aerosol optical thickness, averaged for days having at least 10 clear-sky measurements.

determined by the regression line for the corresponding SZA. Daytime mean TRE was computed as the average of instantaneous TRE values. Fig. 8 shows a comparison between TRE at the surface and SRE in the atmosphere for each month from May to September. It follows that absorption by smoke in the atmosphere contributes substantially to the reduction of solar radiation at the surface, especially in July and August when SRE accounts for about one third of TRE in magnitude.

6. Conclusions

Smoke aerosols produced by fires modify the earth's radiation budget. Until now, studies dealing with smoke radiative effect (SRE) have focused on the top of the atmosphere in tropical regions. This study investigates SRE, the amount of solar radiation absorbed by smoke in the atmosphere, over a boreal forest region in western Canada. A new method is proposed that does not

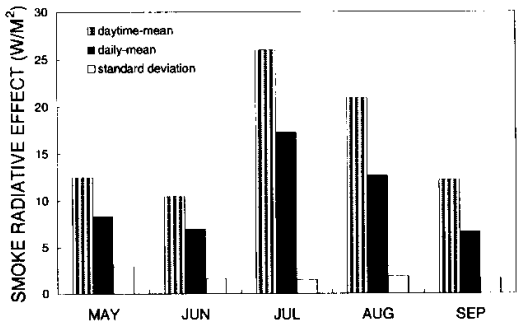

Fig. 6. Monthly mean value of SRE averaged over 24 h (daily-mean) and over the daylight hours (daytime-mean) in the summer months of 1994. The short bars denote the standard deviation of the monthly mean value of SRE.

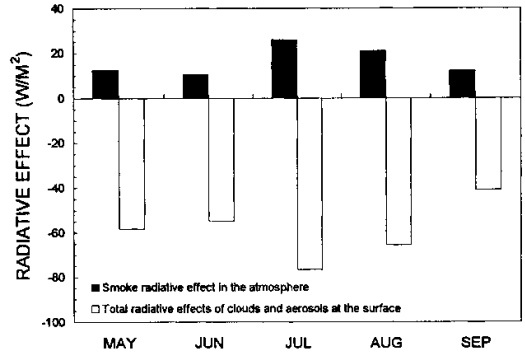

Fig. 8. Comparison of monthly and daytime mean value of TRE at the surface and SRE in the atmosphere.

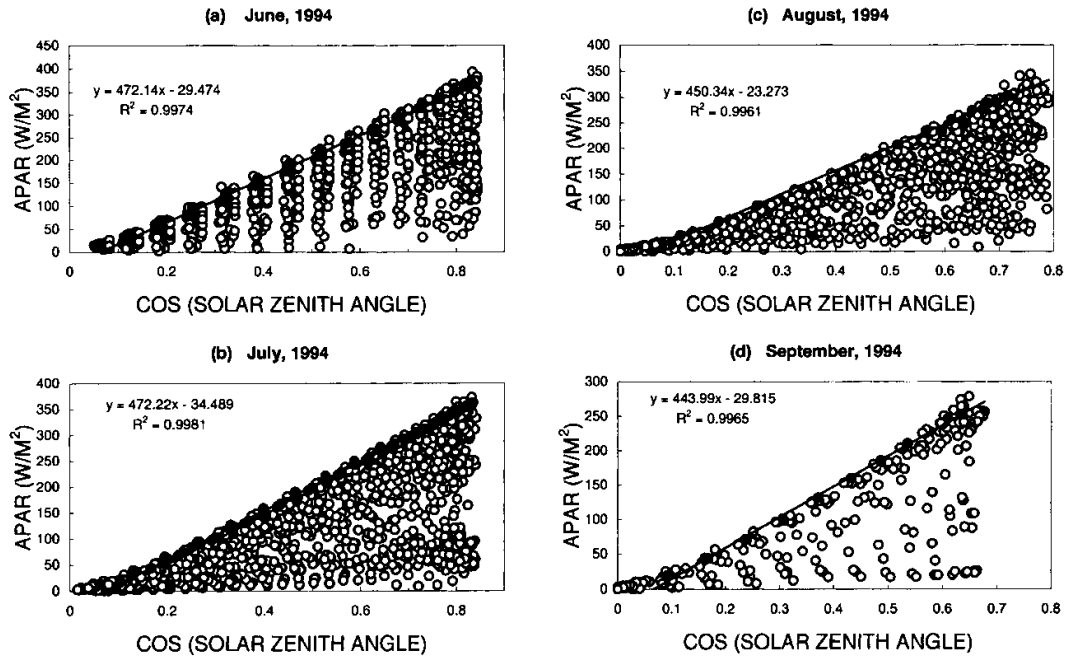

Fig. 7. Surface-observed instantaneous APAR plotted as a function of the cosine of the solar zenith angle. The straight lines are linear regressions of the clear sky measurements (solid points) without the influence of smoke. Also given in the plots are the regression equations and the squares of the linear correlation coefficient of the regression.

require measurements of aerosol optical properties but observations of TOA reflection and surface transmission.

The study is limited to a visible spectral band (400–700 nm) which is often referred to as photosynthetically active radiation (PAR). By virtue of a satellite algorithm (Li and Moreau, 1996) that retrieves surface absorbed PAR (APAR), SRE can be distinguished from the radiative effects of other agents. The algorithm was first validated under a range of sky conditions: clear, smoky and cloudy days. It was found that the estimated fluxes are in good agreement with surface observations for both clear and cloudy days. For smoky days, the estim-

ates are generally greater than the observations. With aerosol corrections, the two fall again into a good agreement. This finding suggests that SRE can be determined simply as the difference between observed and estimated APAR without correction for smoke aerosol. Following this idea, instantaneous, daily and monthly mean SRE values were calculated. At the peak of the burning season, in July 1994, the monthly *daytime* mean atmospheric SRE reaches 26.0 W m^{-2}. This is a significant amount in comparison to the total radiative effect of both clouds and aerosols in reducing surface APAR of 76.7 W m^{-2}, and to the monthly mean APAR of 132.6 W m^{-2}. However, when compared to the SRE in the tropics, these values are considerably smaller. For example, Li (1998) found that during the peak burning season in some tropical regions, smoke may lower monthly and *daily* mean total solar radiation by as much as 100 W m^{-2}, which is equivalent approximately to 110 W m^{-2} in terms of daytime mean APAR.

7. Acknowledgments

The PAR measurements employed in the study were made by two BOREAS science teams led by H. McCaughey at Queen's University and by E. Jelinski at the University of Nebraska, Lincoln. B. L. Markham and his colleagues at NASA/GSFC operated instruments observing aerosols. GOES satellite imagery data were processed by a group led by E. Smith at Florida State University. All the data were made available through the BOREAS Information System (BORIS) administrated by the NASA/GSFC. S. Nadon and A. Trishchenko provided some assistance in the registration and calibration of GOES imagery. The work is supported partially by the US Department of Energy under an Atmospheric Radiation Measurement (ARM) grant DE-FG02–97ER2361.

REFERENCES

Charlson, R. J. and J. Heintzenberg (eds.), 1995. *Aerosol forcing of climate.* John Wiley, Chichester.

Christopher, S. A., D. V. Vulcan, J. Chou and R. M. Welch, 1996. First estimates of the radiative forcing of aerosols from biomass burning using satellite data. *J. Geophys. Res.* **101**, 21,265–21,273.

Chylek, P. and J. Wong, 1995. Effect of absorbing aerosols on global radiation budget. *Geophy. Res. Lett.* **22**, 929–931.

Gu, J. and E. Smith, 1997. High resolution estimates of total solar and PAR surface fluxes over large scale BOREAS study area from GOES measurements. *J. Geophys. Res.* **102**, 29,685–29,705.

Hansen, J., M. Sato, A. Lacis and R. Ruedy, 1997. The missing climate forcing. *Phil. Trans. R. Lond. B.* **352**, 231–240.

Hobbs, P. V., J. S. Reid, R. A. Kotchenruther, R. J. Ferek and R. Weiss, 1997. Direct radiative forcing by smoke from biomass burning. *Science* **275**, 1776–1778.

Intergovernmental Panel on Climate Change, 1995. *Climate change 1995. The science of climate change*, edited by J. T. Houghton et al. Cambridge University Press, Cambridge, UK, pp. 572.

Iqbal, M. *An introduction to solar radiation.* Academic Press, New York, 390 pp., 1983.

Kaufman, Y. J. and R. S. Fraser, 1997. The effects of smoke particles on clouds and climate forcing. *Science* **277**, 1636–1639.

Li, Z., 1998. Influence of absorbing aerosols on the inference of solar surface radiation budget and cloud absorption. *J. Climate* **11**, 5–17.

Li, Z., J. Cihlar, L. Moreau, F. Huang and B. Lee, 1997a. Monitoring fire activities in the boreal ecosystem. *J. Geophys. Res,* **102**, 29,611–29,624.

Li, Z., L. Moreau and J. Cihlar, 1997b. Estimation of the photosynthetically active radiation absorbed at the surface over the BOREAS region. *J. Geophy. Res.* **102**, 29,717–29,727.

Li, Z. and L. Moreau, 1996. A new approach for remote sensing of canopy absorbed photosynthetically active radiation, I: Total Surface Absorption. *Rem. Sens. Environ.* **55**, 175–191.

Markham, B. L., J. S. Schafer, B. N. Holben and R. N. Halthore, 1997. Atmospheric aerosols and water vapor characteristics over north central Canada during BOREAS. *J. Geophys. Res.* **102,** 29737–29745.

Minnis, P., W. L. Smith, D. P. Garber, J. K. Ayers and D. R. Doelling, 1995. Cloud properties derived from GOES-7 for spring 1994 ARM intensive observation period using version 1.0.0 of ARM satellite data analysis program. *NASA Reference Publication* 1366, 58 pp.

Penner, J. E., R. E. Dickinson and C. A. O'Neill, 1992. Effects of aerosol from biomass burning on the global radiation budget. *Science* **256**, 1432–1434.

Radke, L. F., D. A. Hegg, J. H. Lyons, C. A. Brock, P. V. Hobbs, R. Weiss and R. Rasmussen, 1988. Airborne measurements on smoke from biomass burning. *Aerosols and Climate*, edited by P. V. Hobbs and M. P. McCormick, pp. 411–422. Hampton, VA, Deepak Press.

Schwartz, S. E. and M. O. Andreae, 1996. Uncertainties

in climate change caused by aerosols. *Science* **272**, 1121–1122.

Sellers, P., F. Hall, H. Margolis, B. Kelly, D. Baldocchi, G. den Hartog, J. Cihlar, M. G. Ryan, B. Goodison, P. Crill, K. J. Ranson, D. Lettenmaier and D. E. Wickland, 1995. The boreal ecosystem-atmosphere study (BOREAS). An overview and early results from the 1994 field year. *Bull. Am. Meteorol. Soc.* **76**, 1549–1577.

Stocks, B. J. 1996. Monitoring large-scale forest fire behavior in northeastern Siberia using NOAA-AVHRR satellite imagery. In *Biomass burning and climate change*, edited by J. S. Levine, pp. 802–807. MIT press, Cambridge, Mass.

Trishchenko, A. and Z. Li, 1998. Use of ScaRaB measurements for validating a GOES-based TOA radiation product. *J. Appl. Meteor.* **37**, 591–605.

WCP-12, 1986. *A preliminary cloudless standard atmosphere for radiation computation.* World Climate Program, available from the World Meteorological Organization, Geneva, Switzerland, 53pp.